Preprint
UCRL-JC-135190

An Analysis of Gas Pressure Forming of Superplastic AL 5083 Alloy

C. K. Syn, M. J. O'Brien, D. R. Lesuer, O. D. Sherby

This article was submitted to
LIMAT-2001 International Conference on Light Materials for
Transportation Systems, Pusa, Korea, May 6-10, 2001

May 4, 2001

This work was performed under the auspices of the United States Department of Energy by the University of California, Lawrence Livermore National Laboratory under contract No. W-7405-Eng-48.

AN ANALYSIS OF GAS PRESSURE FORMING OF SUPERPLASTIC AL 5083 ALLOY

C.K. Syn, M.J. O'Brien*, D.R. Lesuer, and O.D. Sherby**

Lawrence Livermore National Laboratory, Livermore, CA 94551, USA
* Now at The Aerospace Corp., Los Angeles CA 90009, USA
** Stanford University, Dep't of Mat'ls Science and Eng., Stanford CA 94305, USA

ABSTRACT

Al 5083 disks of a superplastic forming grade were gas-pressure formed to hemispheres and cones at constant forming pressures with and without back pressure. The forming operation was performed using an in-house designed and built biaxial forming apparatus. The temporal change of dome heights of the hemispheres and cones were measured for the different forming and back pressures applied. The flow stresses and strain rates developed at the top of the dome during the forming step were shown to closely follow the flow stress – strain rate relationship obtained from the strain rate change tests performed at the same temperature using uniaxial tensile samples.

1. INTRODUCTION

Recent interest in lightweight and inexpensive alloys for transportation sytems has attracted attentions to aluminum - magnesium alloys. Al 5083 alloy, because of its good weldability, reasonably high corrosion resistance and high strength with reasonable ductility, has been one of such alloys. Large ductility required in forming engineering parts with contoured geometry has led to development of superplastic grade of the alloy [1-4]. Deformation behavior and microstructural evolution of the superplastic Al 5083 has been extensively investigated for tensile deformation [1-8] and the deformation behavior has been modeled for uniaxial tension tests [6, 8] and biaxial forming of rectangular pans [7, 8]. The purpose of the present study is to investigate the deformation behavior during equi-biaxial forming of a commercial superplastic Al 5083 alloy using hemispherical and conical dies.

2. EXPERIMENTAL AND ANALYSIS PROCEDURES

2.1 Material

High-purity superplastic forming (SPF) grade Al 5083-O alloy (Sky Aluminum's Alnovi-1) sheets of nominal 2.5 mm thickness were obtained and the supplier's composition is compared in Table 1with that of standard non-SPF grade. The room temperature tensile properties of 297 MPa tensile strength, 145 MPa yield strength, and 20% elongation were claimed by the supplier of the SPF grade.

Table 1. Composition (in wt. %) of the SPF 5083 alloy used and the standard 5083 alloy

	Si	Fe	Cu	Mn	Mg	Cr	Zn	Ti	Al
Std 5083	0.4 Max	0.4 Max	0.1 Max	0.4-1.0	4.0-4.9	0.05-0.2	0.25Max	0.15 Max	Bal.
Alnovi-1 SPF 5083	0.05	0.05	Tr.	0.69	4.58	0.12	Tr.	0.01	Bal.

2.2 Uniaxial Tensile Tests

The SPF grade material was characterized first with uniaxial tensile tests at elevated temperatures in argon gas atmosphere by strain rate jump tests and constant strain-rate tests to failure. A typical strain-rate change test employed nine different true strain rates from the lowest strain rate of $1x10^{-4}$ s^{-1} through $3x10^{-4}$, $5x10^{-4}$, $1x10^{-3}$, $2x10^{-3}$, $3.5x10^{-3}$, $6x10^{-3}$, $1x10^{-2}$ s^{-1} to the highest strain rate of $2x10^{-2}$ s^{-1}. If the specimen did not fail at the highest strain-rate, several cycles of the nine strain rates were repeated until it failed as shown in Fig. 1. The strain rate jump tests used were also described elsewhere [9].

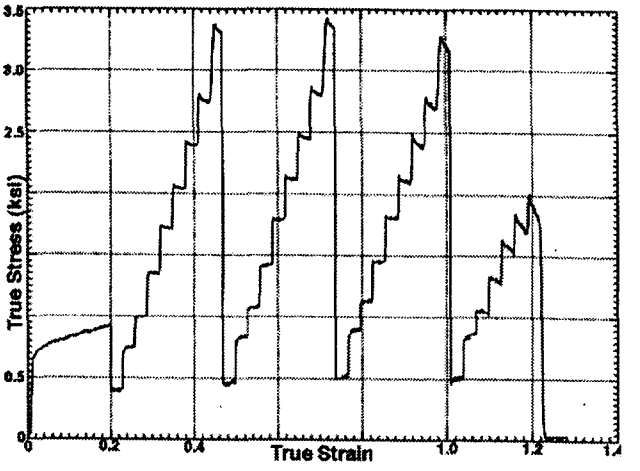

Fig. 1. Example of strain rate change tests. After the initial strain of 0.2 at $5x10^{-4}$ s^{-1}, the strain rate was changed step by step from $1x10^{-4}$ s^{-1} to $2x10^{-2}$ s^{-1}, and the cycle was repeated until the specimen failed.

2.3 Biaxial Gas-Pressure Forming Tests

The forming apparatus was mainly consisted [10], of i) forming die assembly ii) loading mechanism to provide the support for the die assembly and the compressive force to keep the dies closed, iii) heating furnace around the die assembly, iv) pressure control panel which delivers argon gas to the die assembly, and v) data acqusition system recording forming pressure, back pressure, dome height of the specimen being formed, and temperature history.

The die assembly shown in Fig. 2 is comprised of three major components: upper die, lower die, and upper extension. The upper and lower dies made of Inconel 625 alloy. The upper extension made of stainless steel 304 houses linear voltage displacement transducer (LVDT). The tip of the LVDT is connected to a thin hollow alumina rod that is in contact with the test specimen. When the specimen bulges up, the alumina rod is pushed up and its displacement is mesaured by LVDT. Specimen temperature is monitored through two thermocouples placed in the upper die T.C. ports. Forming pressure is provided by pressurizing the lower die below the specimen. The upper extension is pressurized when back pressure is used. The upper die cavity determines the shape of the formed parts. Two cavity designs, hemisperical and conical, were used. The diameter of the hemispherical and conical dies was 50 mm. The apex angle, α, of the conical die was 42.46°.

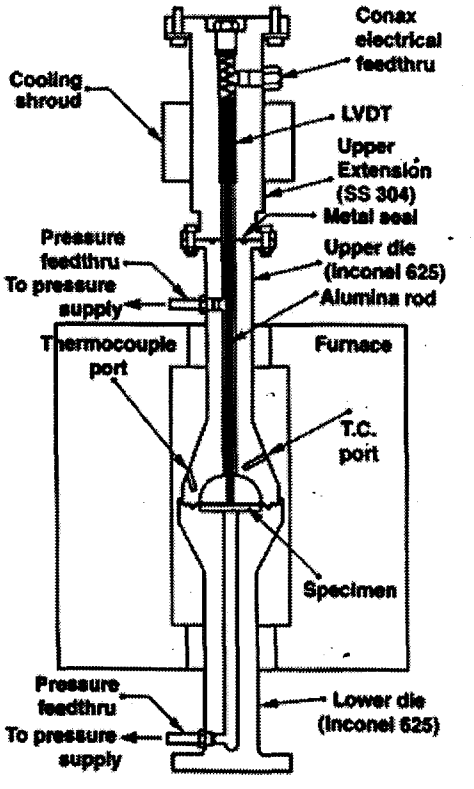

Fig. 2. Die assembly of the superplastic forming apparatus using gas pressure

Some of the specimens were gridded with a square array of touching circles of 2.5 mm diameter. Prior to forming, both sides of the specimen were sprayed with boron nitride powder as a releasing compound. The dies were preheated to the forming temperature. Once the die temperature equilibrated, the furnace was opened and the specimen was inserted in the lower die. This procedure minimized possible static grain growth in the material. The specimen dimensions were 78.7 mm diameter and 2.5 mm thick. When the specimen stabilized at the forming temperature, usually within 5 minutes, a clamping force up to 1360 kg was applied at about 225 kg/min to form the pressure seal. When back pressure was used, argon gas was admitted into both the upper and lower dies and an equal gas pressure was initially applied. The specimen started to form once the gas pressure began to increase in the lower die. A forming operation was terminated either when the predetermined dome height was reached or when the forming pressure started to drop rapidly because of gas leak through holes developed in the specimen.

2.4 Data Analysis

For analysis of the superplastic forming behavior, the disk specimens were assumed to bulge to spherical membranes of uniform thickness. An applied pressure, P, in a hemispherical die of radius R_o would deform a disk specimen of the initial thickness t_o into a spherical membrane of radius, ρ. The membrane would thin to a uniform thickness, t, as shown schematically in Fig. 3. By measuring the dome height H_D of the membrane, and assuming the volume constancy of the material, one can calculate the radius ρ, thickness t, strain ε, strain rate $\dot{\varepsilon}$, and shell stress σ, of the membrane using the following equations.

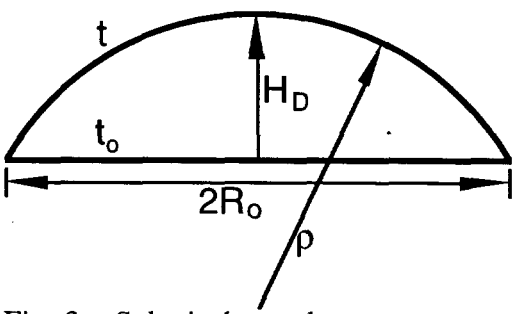

Fig. 3. Spherical membrane geometry assumed in stress analysis of the gas-pressure formed in hemispherical die

$$\rho = (R_o^2 + H_D^2)/2H_D \qquad (1)$$

$$t = R_o^2 \cdot t_o/(2\rho \cdot H_D) \qquad (2)$$

$$\varepsilon = \ln (t / t_o) \qquad (3)$$

$$\dot{\varepsilon} = -\dot{H}_D /r \qquad (4)$$

$$\sigma = P\,\rho/2t \qquad (5)$$

where $\dot{H}_D$ is the temporal change rate of the dome height.

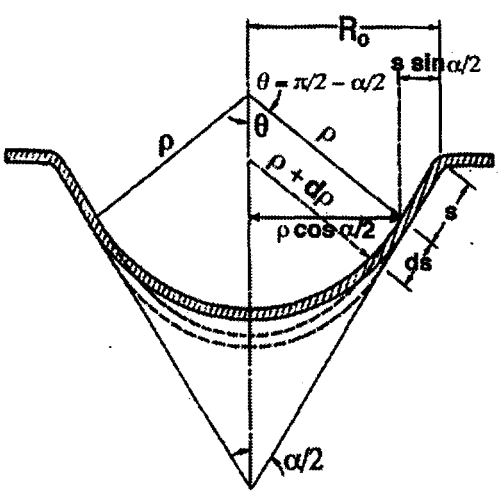

Fig. 4. Stress analysis of the gas-pressure formed in conical die. Spherical membrane geometry assumed after the bulging membrane touches the inner wall of the conical die.

For the analysis of forming behavior in the conical die, Eqs. (1) to (5) can be used until the membrane touches the internal surface of the cone. Once the bulging membrane contacts the cone internal surface, the material in contact was assumed to stick to the die, but in the crown (uncontacted) region it was assumed to continue bulging spherically and thinning uniformly, as proposed by Ghosh and Hamilton [11]. Adopting the relationship between the thickness and meridional strain derived by Ghosh and Hamilton to the present cone geometry with the apex angle $\alpha = 42.46°$, the radius and thickness of the crown region were found given by the following equations.

$$\rho = 1.1538 - 0.5479 \cdot H_D \quad (6)$$

$$t = t_C \cdot (\rho/\rho_C)^{1.8250} \quad (7)$$

where H_D is the dome height of the crown region measured from the surface of initial unbulged specimen, while t_C and ρ_C are the thickness and radius of the membrane at the initial contact. Once the radius and thickness of the crown region are determined, the strain, strain rate, and stress can be calculated using Eqs. (3) to (5).

3. RESULTS AND DISCUSSIONS

Preliminary results of forming tests using hemisperical and conical dies run at 520°C and the uniaxial tensile tests performed at the same temperature are described in this report.

3.1 Uniaxial Tensile Stress - Strain-Rate Relationship

The uniaxial tensile strain-rate jump tests were performed at 520°C. Fig. 1 shows the tensile flow stress - strain-rate curves for the first and third cycles of strain-rates used in the test. At the lower strain-rate range, the material shows a strain-rate sensitivity of m=0.5 indicating deformation by grain boundary sliding mechanism. At higher strain rates, the sensitivity decreases indicating gradual transition to different deformation mechanisms.

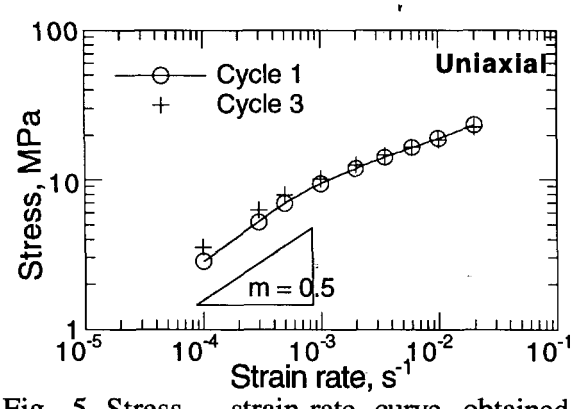

Fig. 5 Stress - strain-rate curve obtained from uniaxial tensile strain-rate jump tests

3.2 Gas-Pressure Forming Behavior

Forming tests with the dies were also performed at 520°C. Each specimens was formed at a constant pressure by rapidly increasing the pressure to a prescribed level. At low level pressures, deformation of the specimen during the pressure rise was negligible, while for high level forming pressures, it was not negligible. Fig. 6 illustrates examples of forming pressure profiles used in hemisperical die forming. Fig.7 illustrates examples of conical die forming with application of back pressure where P_F and P_B represent the pressures in the lower and upper die respectively, and ΔP represents the net forming pressure.

Figs. 8 and 9 show the corresponding dome height profiles measured under the applied forming pressures. Fig. 9 includes the dome height profiles of three other specimens (#11, #14, and #15) which were formed at 0.86, 1.6, and 0.58 MPa respectively in addition to the specimens represented in Fig. 7. One can see from Figs. 8 and 9 that the level of dome height achieved is higher for the specimens formed in conical die and highest in the specimens formed with back pressure. It can be seen also that the rates of dome height change (dH_D/dt) are faster for specimens formed at higher pressure levels.

Figs. 10 and 11 show the calculated shell stresses using Eq. (5) plotted against the dome heights measured for both sets of specimens formed in hemispherical and conical dies. Both in hemispherical and conical die formings, specimens seem to have formed at rather stable or roughly constant stress levels for the dome height range of 8 mm to 22mm, although the stress increases gradually as the dome height increases. The stress rises faster and higher under the higher forming pressure.

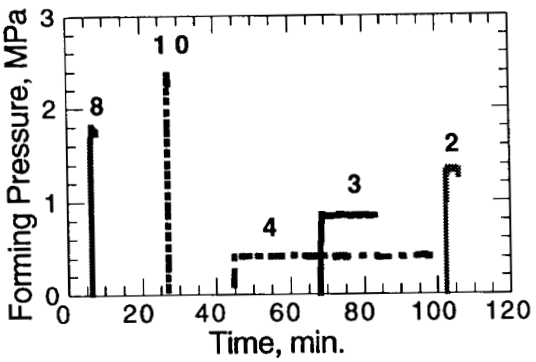

Fig. 6. Pressure profiles used in hemispherical die forming. Numerals on represent specimen numbers

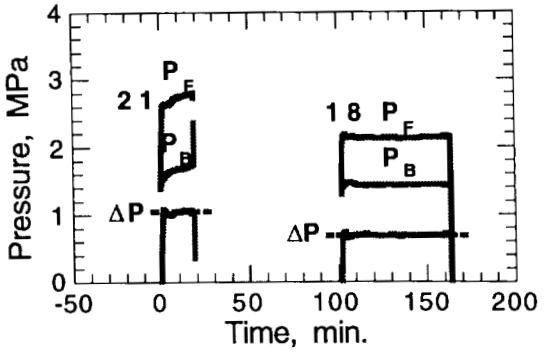

Fig. 7.Pressure profiles used in conical die forming with back pressure. P_F, P_B and ΔP represent the forming, back, and net pressures.

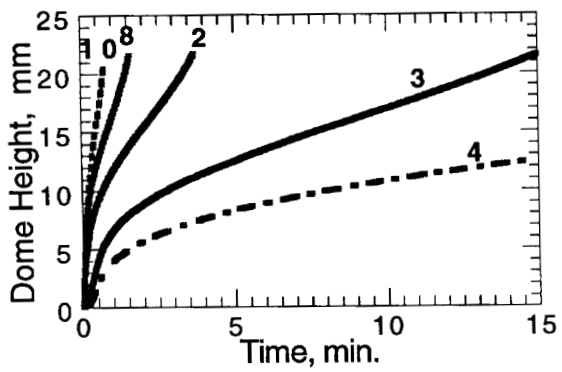

Fig. 8. Dome height profiles for hemispherical die formed specimens represented in Fig. 6.

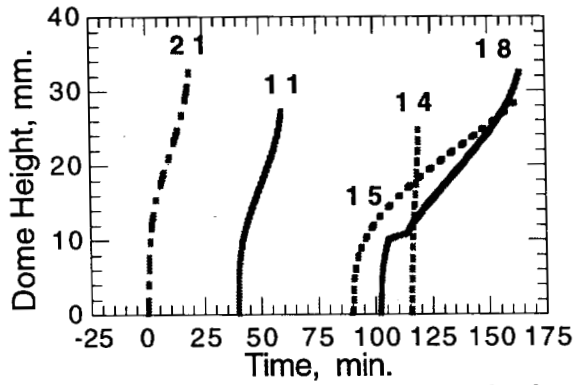

Fig. 9. Dome height measured for specimens represented in Fig. 7 and other specimens formed without back pressure.

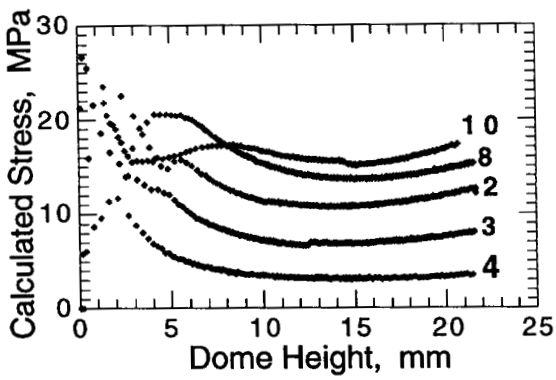

Fig. 10. Calculated shell stress - dome height curves for hemispherical die formed specimens shown in Fig. 8.

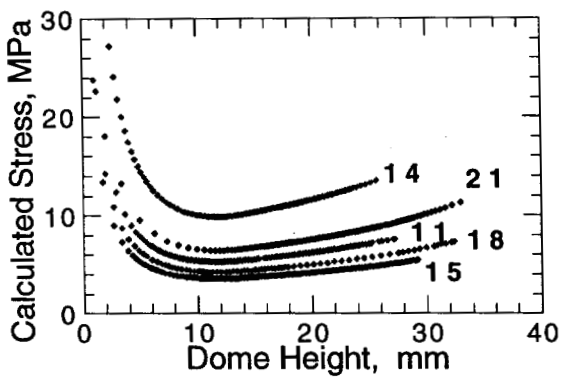

Fig. 11. Calculated shell stress - dome height curves for conical die formed specimens represented in Fig. 9.

Figs. 12 and 13 illustrate the stress -strain-rate relationships obtained in both sets of forming tests. The stresses and strain rates calculated for the dome heights greater than 5 mm were plotted and compared with the results of the uniaxial tensile tests shown in Fig. 5. The calculated stresses are shown as blobs of datapoints in Figs. 12 and 13. Specimens (# 4, 3, 2 and 15) formed at low forming pressures, the forming characteristics coincide with the uniaxial

tensile plastic behavior, while at the higher forming pressure, specimens (#10, 8, and 14) exhibit lower stresses than the uniaxial tensile stresses.

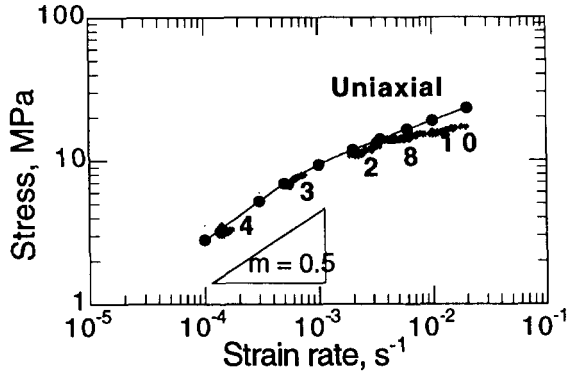

Fig. 12. Stress - strain-rate relationships for specimens formed in hemispherical die compared with the uniaxial test results

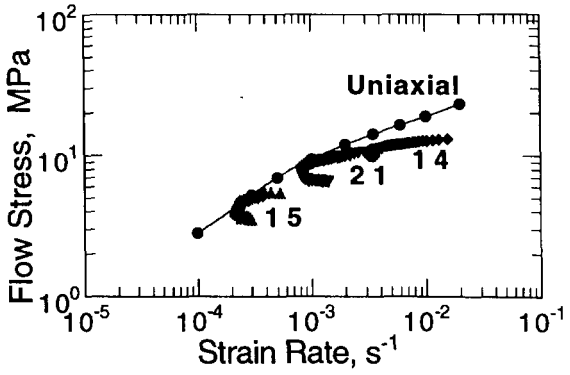

Fig. 13. Stress - strain-rate relationships for specimens formed in conical die compared with the uniaxial test results

4. CONCLUDING REMARKS

Gas pressure forming of SPF grade Al 5083 into hemi-spherical and conical dies was performed at 520°C and variable or constant gas pressures with or without back pressure. The stress – strain-rate relationship was close to the uniaxial tensile stress – strain-rate relation. Additional metallographic investigations of the tested specimens and modeling by finite element method (FEM) were performed. Findings include: (i) high volume fractions of cavitation measured in the dome areas; (ii) the thickness at the peak of dome predicted from Eq. (2) or (7) is close to the measured thickness; (iii) FEM modeling by NIKE 2D code closely simulates the thinning behavior of the material during forming. The additional findings will be examined further in a future report.

ACKNOWLEDGEMENT

This work was performed under the auspices of the United States Department of Energy by the Lawrence Livermore National laboratory under Contract No. W-7405-ENG-48.

REFERENCES

1. H. Iwasaki et al., in Superplasticity in Advanced Materials, S. Hori, M. Tokizane and N. Furushiro, eds., Japan Society for Research on Superplasticity (1991), pp. 447-452.
2. H. Imamura and N. Ridley, ibid, pp. 453-458.
3. J.S. Vetrano et al., in "Superplastic Behavior in a Commercial 5083 Aluminum Alloy", Scripta Metall. Mater., 30 (1994), pp. 565-570.
4. R. Verma, A.K. Ghosh, S. Kim and C. Kim, Mat. Sci. Eng. A191 (1995), pp. 143-150.
5. R. Verma et al, Metall. Mater Trans. A, 27A (1996), pp. 1889-1898,
6. P.A. Friedman and A.K. Ghosh, ibid, pp. 3827-3839.
7. R. Verma et al., J. Mat'ls Eng. Performance, 4 (1995), pp. 543-550,
8. M.A. Khaleel et al., Int'l J. Plasticity, 14 (1998), pp. 1133-1154,
9. Lesuer et al,. in Superplasticity in Advanced Materials, S. Hori, M. Tokizane and N. Furushiro, eds., Japan Society for Research on Superplasticity (1991), pp. 139-144.
10. S.L. Stoner et al., LLNL Report UCRL-JC-118229 (1994).
11. A.K. Ghosh and C.H. Hamilton, Metall. Trans. A, 11A (1980), pp. 1915-1918.